

22 **Abstract:** Forecasting the impacts of climate change on *Aedes*-borne viruses—especially
23 dengue, chikungunya, and Zika—is a key component of public health preparedness. We apply an
24 empirically parameterized Bayesian transmission model of *Aedes*-borne viruses for the two
25 vectors *Aedes aegypti* and *Aedes albopictus* as a function of temperature to predict cumulative
26 monthly global transmission risk in current climates, and compare with projected risk in 2050
27 and 2080 based on general circulation models (GCMs). Our results show that if mosquito range
28 shifts track optimal temperatures for transmission (26-29 °C), we can expect poleward shifts in
29 *Aedes*-borne virus distributions. However, the differing thermal niches of the two vectors
30 produce different patterns of shifts under climate change. More severe climate change scenarios
31 produce proportionally worse population exposures from *Aedes aegypti*, suggesting a strong
32 coupling of climate change and continued emergence of dengue virus; but not from *Aedes*
33 *albopictus* in the most extreme cases, suggesting a less straightforward climate link for
34 chikungunya. Expanding risk of transmission from both mosquitoes will likely be a serious
35 problem, even in the short term, for most of Europe; but significant reductions are also expected
36 for *Aedes albopictus*, most noticeably in southeast Asia and west Africa. Within the next century,
37 nearly a billion people are threatened with new exposure to both *Aedes* spp. in the worst-case
38 scenario; but massive net losses in risk are noticeable for *Aedes albopictus*, especially in terms of
39 year-round transmission, marking a global shift towards more seasonal risk across regions. Many
40 other complicating factors (like mosquito range limits and viral evolution) exist, but overall our
41 results indicate that while climate change will lead to both increased and new exposures to
42 vector-borne disease, partial mitigation may accrue major unanticipated health costs from
43 diseases that are mainly spread by *Aedes albopictus*.

44 **Author Summary:** The established scientific consensus indicates that climate change will
45 severely exacerbate the risk and burden of *Aedes*-transmitted viruses, including dengue,
46 chikungunya, Zika, West Nile virus, and other significant threats to global health security. Here,
47 we show that the story is more complicated, first and foremost due to differences between the
48 more heat-tolerant *Aedes aegypti* and the more heat-limited *Aedes albopictus*. Almost a billion
49 people could face their first exposure to viral transmission from either mosquito in the worst-case
50 scenario, especially in Europe and high-elevation tropical and subtropical regions. On the other
51 hand, while year-round transmission from *Ae. aegypti* is likely to expand (especially in south
52 Asia and sub-Saharan Africa), *Ae. albopictus* loses significant ground in the tropics, marking a
53 global shift towards seasonal risk as the tropics eventually become too hot for transmission.
54 Complete mitigation of climate change to a pre-industrial baseline could protect almost a billion
55 people from arbovirus range expansions; but middle-of-the-road mitigation may actually increase
56 exposure, especially for viruses mainly transmitted by *Aedes albopictus* (such as chikungunya).
57 Mitigating climate change also shifts the burden of both dengue and chikungunya (and
58 potentially other *Aedes* viruses) from higher-income regions back onto the tropics where
59 transmission might otherwise be curbed by rising temperatures.
60

61 **Introduction**

62 Climate change will almost certainly have a profound effect on the global distribution and
63 burden of infectious diseases [1–3]. Current knowledge suggests that the range of mosquito-
64 borne diseases could expand dramatically in response to climate change [4,5]. However, the
65 physiological and epidemiological relationships between mosquito vectors and the environment
66 are complex and often non-linear, and experimental work has showed an idiosyncratic
67 relationship between warming temperatures and disease transmission [6,7]. In addition,
68 pathogens can be vectored by related species, which may be sympatric, or several pathogens may
69 be transmitted by the same vector. Accurately forecasting the potential impacts of climate change
70 on *Aedes*-borne viruses—which include widespread threats like dengue and yellow fever, as well
71 as several emerging threats like chikungunya and Zika—thus becomes a key problem for public
72 health preparedness [4,8,9]. In this paper, we compare the roles and impact of two vectors, *Aedes*
73 *aegypti* (the primary vector of dengue virus around the world) and *Aedes albopictus* (the primary
74 vector of chikungunya virus in its recent emergence), in their contribution to potential
75 transmission landscapes in a changing climate.

76 The intensification and expansion of vector-borne disease is likely to be one of the most
77 significant threats posed by climate change to human health [2,10]. Mosquito vectors are of
78 special concern, due to the global morbidity and mortality from diseases like malaria and dengue
79 fever, as well as the prominent public health crises caused by (or feared from) several recently-
80 emergent viral diseases like West Nile, chikungunya, and Zika. The relationship between climate
81 change and mosquito-borne disease is perhaps best studied, in both experimental and modeling
82 work, for malaria and its associated *Anopheles* vectors. While climate change could exacerbate
83 the burden of malaria at local scales, more recent evidence challenges the “warmer-sicker world”
84 expectation [11,12]. The optimal temperature for malaria transmission has recently been
85 demonstrated to be much lower than previously expected [13], likely leading to net decreases in
86 optimal habitat at continental scales in the coming decades [12].

87 Relative to malaria, less is known about the net impact of climate change on *Aedes*-borne
88 diseases. At a minimum, the distribution of *Aedes* mosquitoes is projected to shift in the face of
89 climate change, with a mix of expansions in some regions and contractions in others, and no
90 overwhelming net global pattern of gains or losses [3,8]. Ecophysiological differences between
91 *Aedes* vector species are likely to drive differences in thermal niches, and therefore different

92 distributions of transmission risk [6,14], now and in the future. The consequences of those range
93 shifts for disease burden are therefore likely to be important, but are challenging to summarize
94 across landscapes and pathogens. Of all *Aedes*-borne diseases, dengue fever has been most
95 frequently modeled in the context of climate change, and several models of the potential future
96 of dengue have been published over the last two decades, with some limited work building
97 consensus among them [4]. Models relating temperature to vectorial capacity (the number of new
98 infectious mosquito bites generated from a human case), and applying general circulation models
99 (GCMs) to predict the impacts of climate change, date back to the late 1990s [5]. A study from
100 2002 estimated that the population at risk (PAR) from dengue would rise from 1.5 billion in
101 1990, to 5-6 billion by 2085, as a result of climate change [15]. A more recent study suggested
102 that climate change alone should increase the global dengue PAR by 0.28 billion by 2050, but
103 accounting for projected changes in global economic development (using GDP as a predictor for
104 dengue risk) surprisingly reduces the projected PAR by 0.12 billion over the same interval [16].
105 Mechanistic models have shown that increases or decreases in dengue risk can be predicted for
106 the same region based on climate models, scenario selection, and regional variability [17].

107 Chikungunya and Zika viruses, which have emerged more recently as a public health
108 crisis, are less well-studied in the context of climate change. A monthly model for chikungunya
109 in Europe, constrained by the presence of *Ae. albopictus*, found that the A1B and B1 scenarios
110 both correspond to substantial increases in chikungunya risk surrounding the Mediterranean [18].
111 A similar modeling study found that dengue is likely to expand far more significantly due to
112 climate change than Zika [9] (though epidemiological differences among these three viruses
113 remain unresolved [19–21]). However, the combined role of climate change and El Niño has
114 already been suggested as a possible driver of the 2016 Zika pandemic's severity [9]. Global
115 mechanistic forecasts accounting for climate change are all but nonexistent for both chikungunya
116 and Zika, given how recently both emerged as public health crises, and how much critical
117 information is still lacking in the basic biology and epidemiology of both pathogens.

118 In this study, we apply a new mechanistic model of the spatiotemporal distribution of
119 *Aedes*-borne viral outbreaks to resolve the role climate change could play in the emergence of
120 diseases like dengue, chikungunya, and Zika. Whereas other mechanistic approaches often rely
121 on methods like dynamic energy budgets to build complex biophysical models for *Aedes*
122 mosquitoes [22,23], and subsequently (sometimes) extrapolate potential epidemiological

123 dynamics [5], our approach uses a single basic cutoff for the thermal interval where viral
124 transmission is possible. The simplicity and transparency of the method masks a sophisticated
125 underlying model that links the basic rate of reproduction R_0 for *Aedes*-borne viruses to
126 temperature, via experimentally-determined physiological response curves for traits like biting
127 rate, fecundity, mosquito lifespan, extrinsic incubation rate, and transmission probability [6]. The
128 model is easily projected into geographic space by defining model-based measures of suitability
129 and classifying each location in space as suitable or not; we take a Bayesian approach in order to
130 take into account uncertainty in the experimental data. This threshold condition defines the
131 temperatures at which transmission is not prevented, rather than the more familiar threshold at
132 which disease invasion is expected ($R_0 > 1$, which cannot be predicted in the absence of
133 assumptions about vector and human population sizes and other factors). We then classify each
134 location by suitability in each month based on already published projections for current climates
135 in the Americas [6].

136 Here, we expand the framework for both *Ae. aegypti* and *Ae. albopictus* to project
137 cumulative months of suitability in current and future (2050 and 2080) climates, and further
138 examine how global populations at risk might change in different climate change scenarios. We
139 explore variation among both climate model selection (general circulation models; GCMs), and
140 potential emissions pathways described in the IPCC 5 (representative concentration pathways;
141 RCPs). In doing so, we provide the first mechanistic forecast for the potential future transmission
142 risk of chikungunya and Zika, which have been forecasted primarily via phenomenological
143 methods (like ecological niche modeling [9]). Our study is also the first to address the seasonal
144 aspects of population at risk for *Aedes*-borne diseases in a changing climate.

145

146 **Methods**

147 ***The Bayesian Model***

148 Our study presents geographic projections of published experimentally-derived mechanistic
149 models of viral transmission by *Aedes aegypti* and *Aedes albopictus*. The approach to fit the
150 thermal responses in a Bayesian framework and combine them to obtain the posterior
151 distribution of R_0 as a function of these traits is described in detail in Johnson *et al.* [7] and the
152 particular traits and fits for *Aedes aegypti* and *Ae. albopictus* are presented in Mordecai *et al.*
153 [24]. In the original modeling study, the underlying data was compiled on transmission of

154 dengue virus by both mosquito species, and the models for each mosquito were subsequently
155 validated on data compiled for three viruses (dengue, chikungunya, and Zika). Once we obtain
156 our posterior samples for R_0 as a function of temperature we can evaluate the probability that R_0
157 > 0 ($\text{Prob}(R_0 > 0)$) at each temperature, giving a distinct curve for each mosquito species. We
158 then define cutoff of $\text{Prob}(R_0 > 0) = \alpha$ to determine our estimates of the thermal niche; here, we
159 use $\alpha = 0.975$. This very high probability allows us to isolate a temperature window for which
160 transmission is almost certainly not excluded; this provides a conservative approach. For *Aedes*
161 *aegypti*, these bounds are 21.3—34.0 °C, and for *Aedes albopictus*, 19.9—29.4 °C.

162

163 *Current & Future Climates*

164 Current mean monthly temperature data was derived from the WorldClim dataset
165 (www.worldclim.org) [25] For future climates, we selected four general circulation models
166 (GCMs) that are most commonly used by studies forecasting species distributional shifts, at a set
167 of four representative concentration pathways (RCPs) that account for different global responses
168 to mitigate climate change. These are the Beijing Climate Center Climate System Model (BCC-
169 CSM1.1); the Hadley GCM (HadGEM2-AO and HadGEM2-ES); and the National Center for
170 Atmospheric Research's Community Climate System Model (CCSM4). Each of these can
171 respectively be forecasted for RCP 2.6, RCP 4.5, RCP 6.0 and RCP 8.5. RCP numbers
172 correspond to increased radiation in W/m^2 by the year 2100, therefore expressing scenarios of
173 increasing severity. (However, even these scenarios are nonlinear over time; for example, in
174 2050, RCP 4.5 is a more severe change than 6.0.) Climate model output data for future scenarios
175 were acquired from the research program on Climate Change, Agriculture, and Food Security
176 (CCAFS) web portal (http://ccafs-climate.org/data_spatial_downscaling/), part of the
177 Consultative Group for International Agricultural Research (CGIAR). We used the model
178 outputs created using the delta downscaling method, from the IPCC AR5. For visualizations
179 presented in the main paper (Figure 2), we used the HadGEM2-ES model, the most commonly
180 used GCM. The mechanistic transmission model was projected onto the climate data using the
181 'raster' package in R 3.1.1. Subsequent visualizations were generated in ArcMap.

182

183 *Population at Risk*

184 To quantify a measure of risk, comparable between current and future climate scenarios, we used
185 population count data from the Gridded Population of the World, version 4 (GPW4) [26],
186 predicted for the year 2015. We selected this particular population product as it is minimally
187 modeled *a priori*, ensuring that the distribution of population on the earth's surface has not been
188 predicted by modeled covariates that would also influence our mechanistic vector-borne disease
189 model predictions. These data are derived from most recent census data, globally, at the smallest
190 administrative unit available, then extrapolated to produce continuous surface models for the
191 globe for 5-year intervals from 2000-2020. These are then rendered as globally gridded data at
192 30 arc-seconds; we aggregated these in R ('raster'³⁰) to match the climate scenario grids at 5
193 minute resolution (approximately 10 km² at the equator). We used 2015 population count as our
194 proxy for current, and explored future risk relative to the current population counts. This
195 prevents arbitrary demographic model-imposed patterns emerging, possibly obscuring climate-
196 generated change. We note that these count data reflect the disparities in urban and rural patterns
197 appropriately for this type of analysis, highlighting population dense parts of the globe.
198 Increasing urbanization would likely amplify the patterns we see, as populations increase overall,
199 and the lack of appropriate population projections at this scale for 30-50 years in the future
200 obviously limits the precision of the forecasts we provide. We thus opted for a most conservative
201 approach. We finally subdivide global populations into geographic and socioeconomic regions as
202 used by the Global Burden of Disease studies (**Figure S1**) [28].

203

204 **Results**

205 The current pattern of suitability suggested by our model based on mean monthly temperatures
206 (**Figure 1**) reproduces the known or projected distributions of dengue [29], chikungunya [30],
207 and Zika [9,31,32] well. For both *Ae. aegypti* and *Ae. albopictus*, most of the tropics is currently
208 optimal for viral transmission year-round, with suitability declining along latitudinal gradients.
209 Many temperate regions are suitable for up to 6 months of the year currently, but outside the
210 areas mapped as "suitable" by previous disease-specific distribution models, or where *Aedes*
211 mosquitoes are established; in some cases, limited outbreaks may only happen when cases are
212 imported from travelers (e.g. in northern Australia, where dengue is not presently endemic but
213 outbreaks happen in suitable regions [17]; or in mid-latitude regions of the United States, where
214 it has been suggested that traveler cases could result in limited autochthonous transmission

215 [31,33]). In total, our model predicts that 6.01 billion people currently live in areas suitable for
216 *Ae. aegypti* transmission at least part of the year (i.e., 1 month or more) and 6.33 billion in areas
217 suitable for *Ae. albopictus* transmission (using mean temperatures).

218 Even by 2050, warming temperatures are expected to produce dramatic expansions of
219 *Aedes* transmission risk (**Figure 2**). For *Aedes aegypti*, the pattern is (visually, even) fairly
220 straightforward: major expansions of one- or two-month transmission risk in temperate regions
221 are paired with expansion of year-round transmission in the tropics, even into the high-elevation
222 regions that were previously protected. *Aedes albopictus* transmission risk similarly expands
223 majorly (more so, even) into temperate regions, especially high latitude parts of Eurasia and
224 North America. But the upper thermal limits to *Aedes albopictus* transmission are passed in
225 many places, producing major reductions in regions of seasonal risk (like North Africa) and
226 year-round suitability (northern Australia, the Amazon basin, central Africa and southern Asia).
227 Whereas the conventional tropical-temperate gradient of mosquito-borne transmission is
228 preserved for *Aedes aegypti*, warming becomes so severe in the tropics that year-round *Aedes*
229 *albopictus* starts to look more unfamiliar, especially in the more extreme climate pathways. By
230 2080, year-round transmission by *Ae. albopictus* is mostly confined to high elevation regions,
231 southern Africa, and the Atlantic coast of Brazil; and even *Aedes aegypti* has begun to lose some
232 core area of year-round transmission in the Amazon basin especially.

233 Globally, our models suggest a net increase in population at risk from *Aedes*-borne virus
234 exposure, closely tracking the global rise in mean temperatures (**Figure 3**). For both mosquitoes,
235 populations at risk of any exposure will experience a major net increase by 2050, on the order of
236 roughly half a billion people; but even then, increases are more severe for *Ae. aegypti* than for
237 *Ae. albopictus*. But by 2080, the differences between the mosquitoes produce a different result:
238 while more severe warming continues to increase exposure for *Ae. aegypti*, up to nearly a billion
239 net new exposures, the most extreme expansions for *Ae. albopictus* are in middle of the road
240 scenarios (RCP 4.5 and 6.0). For year-round exposure, net changes tell an even more different
241 story between the two mosquitoes. For *Ae. aegypti*, warming temperatures lead to a net increase
242 of roughly 100-300 million people in areas of year-round transmission; though in fact, in RCP
243 8.5 by 2080, some parts of the tropics become so warm that even *Ae. aegypti* is no longer able to
244 transmit. But even by 2050 in the mildest scenarios, there are drastic net losses of year-round

245 transmission for *Aedes albopictus*, and these only become more severe – approaching roughly
246 700 million – in the warmest timelines.

247 Breaking these results down by region (**Table 1 & 2**) highlights just how much regional
248 velocity of climate change is likely to determine future disparities in global health. For *Aedes*
249 *aegypti*, the most notable net increases in all transmission risk are in all regions of Europe, with
250 additional notable gains in east Asia, high-elevation parts of central America and east Africa, and
251 the United States and Canada. But increases are expected across the board except in the
252 Caribbean, where minor net losses are expected across scenarios and years. In contrast, for *Aedes*
253 *albopictus*, there are much more regionally-variable changes anticipated. Major gains in Europe
254 are again expected across the board, as well as less significant increases in central America, east
255 Africa and east Asia, and the U.S. and Canada. But major net losses are also expected in several
256 regions, including tropical Latin America, western Africa, south Asia and most of all southeast
257 Asia, with a net loss of nearly 125 million people at risk by 2080 in RCP 8.5. In some cases, as
258 for western Africa and southeast Asia, the difference between RCP 6.0 and 8.5 is on the order of
259 50 and 100 million people respectively, highlighting just how large a (negative) difference minor
260 levels of climate mitigation might make in those regions.

261 For year-round transmission, the patterns are again less straightforward (**Table S1 & S2**),
262 but overall, they highlight a global shift towards more seasonal risk for both mosquitoes,
263 especially in the warmest scenarios. For *Aedes aegypti*, some of the largest net gains in people at
264 risk are expected in southern Africa, with additional notable increases expected in Latin
265 America. But even for *Ae. aegypti*, warming temperatures exceed levels suitable for year-round
266 transmission in some cases; for example, of all pathways, RCP 4.5 leads to the most severe
267 increases in southern Asia. Overall, almost 600 million people will move into areas with year-
268 round suitability for transmission, though the net increase will be much less (**Table S3**). For
269 *Aedes albopictus*, major net losses are expected in south and southeast Asia (totaling more than
270 400 million with the most extreme warming), and additional losses are expected in east Africa
271 and Latin America. Only the southern part of sub-Saharan Africa consistently experiences net
272 gains in year-round transmission risk; but gross increases are also expected in several regions,
273 most of all east Africa, moving roughly 250 million people into areas of year-round transmission
274 despite nearly triple that number in net losses.

275 We finally consider the idea of “first exposures” separately (gross gains, not accounting
276 for losses), which may be the most epidemiologically significant form of exposure. As the 2005
277 epidemic of chikungunya in India and the 2015 pandemic of Zika virus in the Americas
278 highlight, arboviral introductions into naïve populations can produce atypically severe outbreaks
279 on the order of millions of infections. We rank regions by these first exposures (**Table 3**), and we
280 find that consistently the most significant new exposures are expected in Europe and east Africa
281 for both mosquitoes, confirming fears that both regions may—as a consequence of climate
282 change, if not currently—be at risk from these types of black swan outbreaks. With an outbreak
283 of chikungunya virus in Kenya concurrent to the development of this study, these results seem
284 especially prescient.

285

286 **Discussion**

287

288 The dynamics of mosquito-borne illnesses are climate driven, and current work mostly suggests
289 that climate change will create massive opportunities for the expansion and intensification of
290 *Aedes*-borne illnesses within the next century. Especially since the emergence of Zika in the
291 Americas, many modeling studies have anticipated climate-driven emergence of dengue and
292 chikungunya at higher latitudes [34,35] and higher elevations [36,37]. Within this literature,
293 there have been several global studies of potential expansion [9,17,38], as well as significant
294 focused interest in North America and Europe (perhaps reflecting geographic biases in research
295 priorities and research institutions) [39]. The vast majority of this work has suggested that
296 climate change will probably increase the global burden of morbidity and mortality from dengue
297 and chikungunya, and therefore, that mitigation will likely improve global health outcomes
298 [40,41]. Perhaps most concerning are fears that *Aedes*-borne viruses will be introduced into
299 regions that have previously been unsuitable for transmission, given the potential for explosive
300 outbreaks (like Zika in the Americas, or chikungunya in India) when viruses are first introduced
301 into naïve populations [42]. The emergence of a Zika pandemic in the Old World [43], the
302 establishment of chikungunya in Europe beyond small outbreaks [18], or introduction of dengue
303 anywhere the virus (or any given serotype) has not recently been found, is still a critical concern.

304 Overall, our findings support the general view that climate change will produce major
305 expansions of *Aedes*-borne viral transmission risk. However, we also find more nuanced patterns

306 emerging between the two species, and among different climate pathways. The largest increases
307 in population at risk are consistently in Europe, with additional increases in high altitude regions
308 in the tropics (eastern Africa and the northern Andes) and in the United States and Canada.
309 These increases are expected not only for occasional exposure, but also for longer seasons of
310 transmission, especially for *Ae. aegypti*. But mosquitoes are adapted to their existing climatic
311 range, and while viral transmission will surely track warming temperatures into new places over
312 some intervals, there is no reason to think warming temperatures would produce a unilateral and
313 indefinite increase in disease transmission. Here we show that in the tropics, for *Aedes albopictus*
314 in particular, more extreme climate pathways produce warming temperatures that exceed the
315 suitable range for transmission in many parts of the world; and in the long term, even though
316 total exposure may increase from both mosquitoes in our study, we predict a global shift towards
317 seasonal regimes of exposure from *Aedes albopictus* and therefore, probably, chikungunya.

318 As warming temperatures may begin to exceed the upper thermal bounds of transmission,
319 this produces an unexpected problem in terms of climate change mitigation. Total mitigation
320 (down to pre-industrial baselines) would presumably prevent this redistribution of global risk.
321 But partial mitigation of climate change, i.e. less severe RCPs, could keep *Ae. albopictus*
322 mosquitoes especially within optimal thermal ranges for more of the year, and thereby produce
323 worse clinical outcomes. If our model continues to appropriately predict thermal bounds of viral
324 transmission into the future, this suggests a potential tradeoff in global health priorities, where
325 the scenarios that mitigate global dengue exposure, for example, might come with expanded risk
326 of chikungunya. But it is also unlikely that decisions about climate change mitigation will strictly
327 be decided based on global health priorities, given the already insufficient response to curb
328 carbon emissions and keep temperatures below the 2° C target [44]. In light of this, models such
329 as the ones we present here are probably most useful as a means to anticipate possible futures,
330 depending on the degree of mitigation achieved.

331 These global disease futures are inherently and incredibly stochastic, and the degree to
332 which our models correspond to reality depend not only on uncertainty about climate change, but
333 uncertainty about the biotic homogenization process for disease. For example, reductions in
334 transmission may be less prevalent than we expect here, as—even accounting for the velocity of
335 climate change—viruses will probably have sufficient time to adapt to warming temperatures
336 (within whatever evolvability they possess). Increases in transmission risk are also complicated

337 by many factors, such as the presence or absence of *Aedes* mosquitoes, which are also
338 undergoing their own semi-independent range shifts facilitated by both climate change and
339 human movement; our model already describes areas where *Aedes albopictus* and *Ae. aegypti* are
340 absent but could be present in the future (and even now the ranges of these mosquitoes are not
341 static, by any standard). Whether expanding transmission risk leads to future establishment and
342 viral outbreaks depends not only on disease introduction, but also on land use patterns and
343 urbanization at regional scales, a fact that may ultimately buffer some high-elevation regions like
344 the Andes from increased disease risk [45,46].

345 In practice, these models are a first step towards an adequate understanding of potential
346 global health futures, and the forecast horizon of these models will ultimately be determined by a
347 number of confounding factors [47,48]. In particular, the link from transmission risk to clinical
348 outcomes is confounded by other health impacts of climate change, including changing
349 precipitation patterns, socioeconomic development, changing patterns of land use and
350 urbanization, potential vector (and virus) evolution and adaptation to warming temperatures, and
351 changing healthcare and vector management landscapes, all of which covary strongly
352 (potentially leading to nonlinearities). Moreover, human adaptation to climate change will matter
353 just as much as mitigation in determining how risk patterns shift; for example, increased drought
354 stress will likely encourage water storage practices that increase proximity to *Aedes* breeding
355 habitat [49]. Together these will determine the burden of *Aedes*-borne outbreaks, in ways that
356 determine the eventual relevance of the forecasts we present here.

357 These models are certainly not the only ones to address this pressing topic, and different
358 approaches control for data limitations, confounding processes, climate model uncertainty and
359 disease model uncertainty, different concepts of population at risk, and preferences towards
360 experimental, mechanistic, or phenomenological approaches differently. While climate change
361 poses perhaps the most serious growing threat to global health security, the relationship between
362 climate change and worsening clinical outcomes for *Aedes*-borne diseases is unlikely to be
363 straightforward, and no single model will accurately predict the complex process of a global
364 regime shift in *Aedes*-borne viral transmission. Our models only set an outer spatiotemporal
365 bound to where transmission is thermally plausible; climate change is likely to change the risk-
366 burden relationship at fine scales within those zones of transmission in nonlinear ways, such that
367 areas with shorter seasons of transmission could still experience worse overall disease burdens,

368 or vice versa. Combining broad spatial models with finer-scale models of attack rates or outbreak
369 size is a critical step towards bridging scales [43,50], but more broadly, research building
370 consensus between all available models is of paramount importance [51]. This task is not limited
371 to research on dengue and chikungunya; with several emerging flaviviruses on the horizon
372 [52,53], and countless other emerging arboviruses likely to test the limits of public health
373 infrastructure in coming years [54], approaches like ours that bridge the gap between
374 experimental biology and global forecasting can be one of the foundational methods of
375 anticipating and preparing for the “Next Big One.”

376

377 **Acknowledgements**

378 This work was funded by the National Science Foundation (DEB-1518681 to SJR, LRJ, EAM,
379 NSF DEB-1641145 to SJR, and DEB-1640780 to EAM), and CDC grant 1U01CK000510-01:
380 Southeastern Regional Center of Excellence in Vector-Borne Diseases: the Gateway Program, to
381 SJR. This publication was supported by the Cooperative Agreement Number above from the
382 Centers for Disease Control and Prevention. Its contents are solely the responsibility of the
383 authors and do not necessarily represent the official views of the Centers for Disease Control and
384 Prevention. Support was also provided by the Stanford Woods Institute for the Environment
385 ([https:// woods.stanford.edu/research/environmental- venture-projects](https://woods.stanford.edu/research/environmental-venture-projects)), and the Stanford Center
386 for Innovation in Global Health ([http://globalhealth. stanford.edu/research/seed-grants.html](http://globalhealth.stanford.edu/research/seed-grants.html)).
387 Van Savage, Naveed Heydari, Jason Rohr, Matthew Thomas, and Marta Shocket provided
388 helpful discussions on modeling approaches.

389

390 **Author Information**

391 The authors declare no competing interests. Correspondence and requests for materials should be
392 addressed to S.J.R. (sjryan@ufl.edu).

393

394 **Author Contributions**

395 SJR and LJ ran the models, and CJC and SJR ran the analyses. CJC, SJR, EAM, and LJ wrote
396 the manuscript. CJC and SJR made the figures.

397

398 **References**

- 399 1. Hoberg EP, Brooks DR. Evolution in action: climate change, biodiversity dynamics and emerging
400 infectious disease. *Phil Trans R Soc B*. 2015;370: 20130553.
- 401 2. Lafferty KD. The ecology of climate change and infectious diseases. *Ecology*. 2009;90: 888–900.
- 402 3. Escobar LE, Romero-Alvarez D, Leon R, Lepe-Lopez MA, Craft ME, Borbor-Cordova MJ, et al.
403 Declining Prevalence of Disease Vectors Under Climate Change. *Sci Rep*. 2016;6.
- 404 4. Messina JP, Brady OJ, Pigott DM, Golding N, Kraemer MU, Scott TW, et al. The many projected
405 futures of dengue. *Nat Rev Microbiol*. 2015;13: 230–239.
- 406 5. Patz JA, Martens W, Focks DA, Jetten TH. Dengue fever epidemic potential as projected by general
407 circulation models of global climate change. *Environ Health Perspect*. 1998;106: 147.
- 408 6. Mordecai E, Cohen J, Evans MV, Gudapati P, Johnson LR, Lippi CA, et al. Detecting the impact of
409 temperature on transmission of Zika, dengue, and chikungunya using mechanistic models. *PLoS
410 Negl Trop Dis*. 2017;11: e0005568.
- 411 7. Johnson LR, Ben-Horin T, Lafferty KD, McNally A, Mordecai E, Paaijmans KP, et al.
412 Understanding uncertainty in temperature effects on vector-borne disease: a Bayesian approach.
413 *Ecology*. 2015;96: 203–213.
- 414 8. Campbell LP, Luther C, Moo-Llanes D, Ramsey JM, Danis-Lozano R, Peterson AT. Climate
415 change influences on global distributions of dengue and chikungunya virus vectors. *Phil Trans R
416 Soc B*. 2015;370: 20140135.
- 417 9. Carlson CJ, Dougherty ER, Getz W. An ecological assessment of the pandemic threat of Zika virus.
418 *PLoS Negl Trop Dis*. 2016;10: e0004968.
- 419 10. Githeko AK, Lindsay SW, Confalonieri UE, Patz JA. Climate change and vector-borne diseases: a
420 regional analysis. *Bull World Health Organ*. 2000;78: 1136–1147.
- 421 11. Ibelings B, Gsell A, Mooij W, Van Donk E, Van Den Wyngaert S, Domis D, et al. Chytrid
422 infections and diatom spring blooms: paradoxical effects of climate warming on fungal epidemics in
423 lakes. *Freshw Biol*. 2011;56: 754–766.
- 424 12. Ryan SJ, McNally A, Johnson LR, Mordecai EA, Ben-Horin T, Paaijmans K, et al. Mapping
425 physiological suitability limits for malaria in Africa under climate change. *Vector-Borne Zoonotic
426 Dis*. 2015;15: 718–725.
- 427 13. Mordecai EA, Paaijmans KP, Johnson LR, Balzer C, Ben-Horin T, Moore E, et al. Optimal
428 temperature for malaria transmission is dramatically lower than previously predicted. *Ecol Lett*.
429 2013;16: 22–30.
- 430 14. Brady OJ, Golding N, Pigott DM, Kraemer MU, Messina JP, Reiner Jr RC, et al. Global
431 temperature constraints on *Aedes aegypti* and *Ae. albopictus* persistence and competence for dengue
432 virus transmission. *Parasit Vectors*. 2014;7: 338.
- 433 15. Hales S, De Wet N, Maindonald J, Woodward A. Potential effect of population and climate changes
434 on global distribution of dengue fever: an empirical model. *The Lancet*. 2002;360: 830–834.

- 435 16. Åström C, Rocklöv J, Hales S, Béguin A, Louis V, Sauerborn R. Potential distribution of dengue
436 fever under scenarios of climate change and economic development. *Ecohealth*. 2012;9: 448–454.
- 437 17. Williams C, Mincham G, Faddy H, Viennet E, Ritchie S, Harley D. Projections of increased and
438 decreased dengue incidence under climate change. *Epidemiol Infect*. 2016; 1–10.
- 439 18. Fischer D, Thomas SM, Suk JE, Sudre B, Hess A, Tjaden NB, et al. Climate change effects on
440 Chikungunya transmission in Europe: geospatial analysis of vector's climatic suitability and virus'
441 temperature requirements. *Int J Health Geogr*. 2013;12: 51.
- 442 19. Funk S, Kucharski AJ, Camacho A, Eggo RM, Yakob L, Murray LM, et al. Comparative analysis of
443 dengue and Zika outbreaks reveals differences by setting and virus. *PLoS Negl Trop Dis*. 2016;10:
444 e0005173.
- 445 20. Bastos L, Villela DA, Carvalho LM, Cruz OG, Gomes MF, Durovni B, et al. Zika in Rio de Janeiro:
446 assessment of basic reproductive number and its comparison with dengue. *BioRxiv*. 2016; 055475.
- 447 21. Riou J, Poletto C, Boëlle P-Y. A comparative analysis of Chikungunya and Zika transmission.
448 *Epidemics*. 2017;
- 449 22. Kearney M, Porter WP, Williams C, Ritchie S, Hoffmann AA. Integrating biophysical models and
450 evolutionary theory to predict climatic impacts on species' ranges: the dengue mosquito *Aedes*
451 *aegypti* in Australia. *Funct Ecol*. 2009;23: 528–538.
- 452 23. Hopp MJ, Foley JA. Global-scale relationships between climate and the dengue fever vector, *Aedes*
453 *aegypti*. *Clim Change*. 2001;48: 441–463.
- 454 24. Mordecai EA, Cohen JM, Evans MV, Gudapati P, Johnson LR, Lippi CA, et al. Detecting the
455 impact of temperature on transmission of Zika, dengue, and chikungunya using mechanistic models.
456 *PLoS Negl Trop Dis*. 2017;11: e0005568.
- 457 25. Hijmans RJ, Cameron SE, Parra JL, Jones PG, Jarvis A. Very high resolution interpolated climate
458 surfaces for global land areas. *Int J Climatol*. 2005;25: 1965–1978.
- 459 26. Center for International Earth Science Information Network (CIESIN), Columbia University.
460 Gridded Population of the World, Version 4 (GPWv4). [Internet]. US NASA Socioeconomic Data
461 and Applications Center (SEDAC); 2016. Available: [http://sedac.ciesin.columbia.edu/data/set/gpw-](http://sedac.ciesin.columbia.edu/data/set/gpw-v4-population-count-adjusted-to-2015-unwpp-country-totals)
462 [v4-population-count-adjusted-to-2015-unwpp-country-totals](http://sedac.ciesin.columbia.edu/data/set/gpw-v4-population-count-adjusted-to-2015-unwpp-country-totals)
- 463 27. Hijmans RJ, van Etten J. raster: Geographic analysis and modeling with raster data. [Internet]. 2012.
464 Available: <http://CRAN.R-project.org/package=raster>
- 465 28. Moran AE, Oliver JT, Mirzaie M, Forouzanfar MH, Chilov M, Anderson L, et al. Assessing the
466 global burden of ischemic heart disease: part 1: methods for a systematic review of the global
467 epidemiology of ischemic heart disease in 1990 and 2010. *Glob Heart*. 2012;7: 315–329.
- 468 29. Bhatt S, Gething PW, Brady OJ, Messina JP, Farlow AW, Moyes CL, et al. The global distribution
469 and burden of dengue. *Nature*. 2013;496: 504–507.

- 470 30. Nsoesie EO, Kraemer M, Golding N, Pigott DM, Brady OJ, Moyes CL, et al. Global distribution
471 and environmental suitability for chikungunya virus, 1952 to 2015. *Euro Surveill Bull Eur Sur Mal*
472 *Transm Eur Commun Dis Bull.* 2016;21.
- 473 31. Samy AM, Thomas SM, Wahed AAE, Cohoon KP, Peterson AT. Mapping the global geographic
474 potential of Zika virus spread. *Mem Inst Oswaldo Cruz.* 2016;111: 559–560.
- 475 32. Messina JP, Kraemer MU, Brady OJ, Pigott DM, Shearer FM, Weiss DJ, et al. Mapping global
476 environmental suitability for Zika virus. *Elife.* 2016;5: e15272.
- 477 33. Bogoch II, Brady OJ, Kraemer M, German M, Creatore MI, Kulkarni MA, et al. Anticipating the
478 international spread of Zika virus from Brazil. *Lancet Lond Engl.* 2016;387: 335–336.
- 479 34. Ng V, Fazil A, Gachon P, Deuymes G, Radojević M, Mascarenhas M, et al. Assessment of the
480 probability of autochthonous transmission of Chikungunya virus in Canada under recent and
481 projected climate change. *Environ Health Perspect.* 2017;125.
- 482 35. Butterworth MK, Morin CW, Comrie AC. An analysis of the potential impact of climate change on
483 dengue transmission in the southeastern United States. *Environ Health Perspect.* 2017;125: 579.
- 484 36. Acharya BK, Cao C, Xu M, Khanal L, Naeem S, Pandit S. Present and Future of Dengue Fever in
485 Nepal: Mapping Climatic Suitability by Ecological Niche Model. *Int J Environ Res Public Health.*
486 2018;15: 187.
- 487 37. Equihua M, Ibáñez-Bernal S, Benítez G, Estrada-Contreras I, Sandoval-Ruiz CA, Mendoza-Palmero
488 FS. Establishment of *Aedes aegypti* (L.) in mountainous regions in Mexico: increasing number of
489 population at risk of mosquito-borne disease and future climate conditions. *Acta Trop.* 2017;166:
490 316–327.
- 491 38. Tjaden NB, Suk JE, Fischer D, Thomas SM, Beierkuhnlein C, Semenza JC. Modelling the effects of
492 global climate change on Chikungunya transmission in the 21 st century. *Sci Rep.* 2017;7: 3813.
- 493 39. Tjaden NB, Caminade C, Beierkuhnlein C, Thomas SM. Mosquito-borne diseases: advances in
494 modelling climate-change impacts. *Trends Parasitol.* 2017;
- 495 40. O’Neill BC, Done JM, Gettelman A, Lawrence P, Lehner F, Lamarque J-F, et al. The benefits of
496 reduced anthropogenic climate change (BRACE): a synthesis. *Clim Change.* 2018;146: 287–301.
- 497 41. Colón-González FJ, Harris I, Osborn TJ, São Bernardo CS, Peres CA, Hunter PR, et al. Limiting
498 global-mean temperature increase to 1.5–2° C could reduce the incidence and spatial spread of
499 dengue fever in Latin America. *Proc Natl Acad Sci.* 2018;115: 6243–6248.
- 500 42. Lucey DR, Gostin LO. The emerging Zika pandemic: enhancing preparedness. *Jama.* 2016;315:
501 865–866.
- 502 43. Siraj AS, Perkins TA. Assessing the population at risk of Zika virus in Asia—is the emergency really
503 over? *BMJ Glob Health.* 2017;2: e000309.
- 504 44. Hagel K, Milinski M, Marotzke J. The level of climate-change mitigation depends on how humans
505 assess the risk arising from missing the 2 C target. *Palgrave Commun.* 2017;3: 17027.

- 506 45. Grau HR, Aide TM, Zimmerman JK, Thomlinson JR, Helmer E, Zou X. The ecological
507 consequences of socioeconomic and land-use changes in postagriculture Puerto Rico. *AIBS Bull.*
508 2003;53: 1159–1168.
- 509 46. Li Y, Kamara F, Zhou G, Puthiyakunnon S, Li C, Liu Y, et al. Urbanization increases *Aedes*
510 *albopictus* larval habitats and accelerates mosquito development and survivorship. *PLoS Negl Trop*
511 *Dis.* 2014;8: e3301.
- 512 47. Getz WM, Marshall CR, Carlson CJ, Giuggioli L, Ryan SJ, Romañach SS, et al. Making ecological
513 models adequate. *Ecol Lett.* 2018;21: 153–166.
- 514 48. Petchey OL, Pontarp M, Massie TM, Kéfi S, Ozgul A, Weilenmann M, et al. The ecological
515 forecast horizon, and examples of its uses and determinants. *Ecol Lett.* 2015;18: 597–611.
- 516 49. Beebe NW, Cooper RD, Mottram P, Sweeney AW. Australia’s dengue risk driven by human
517 adaptation to climate change. *PLoS Negl Trop Dis.* 2009;3: e429.
- 518 50. Perkins TA, Siraj AS, Ruktanonchai CW, Kraemer MU, Tatem AJ. Model-based projections of
519 Zika virus infections in childbearing women in the Americas. *Nat Microbiol.* 2016;1: 16126.
- 520 51. Carlson CJ, Dougherty E, Boots M, Getz W, Ryan S. Consensus and conflict among ecological
521 forecasts of Zika virus outbreaks in the United States. *Sci Rep.* 2018;8: 4921.
- 522 52. Evans MV, Murdock CC, Drake JM. Anticipating Emerging Mosquito-borne Flaviviruses in the
523 USA: What Comes after Zika? *Trends Parasitol.* 2018;
- 524 53. Olival K, Willoughby A. Prioritizing the “Dormant” Flaviviruses. *EcoHealth.* 2017;14: 1–2.
- 525 54. Gould EA, Higgs S. Impact of climate change and other factors on emerging arbovirus diseases.
526 *Trans R Soc Trop Med Hyg.* 2009;103: 109–121.

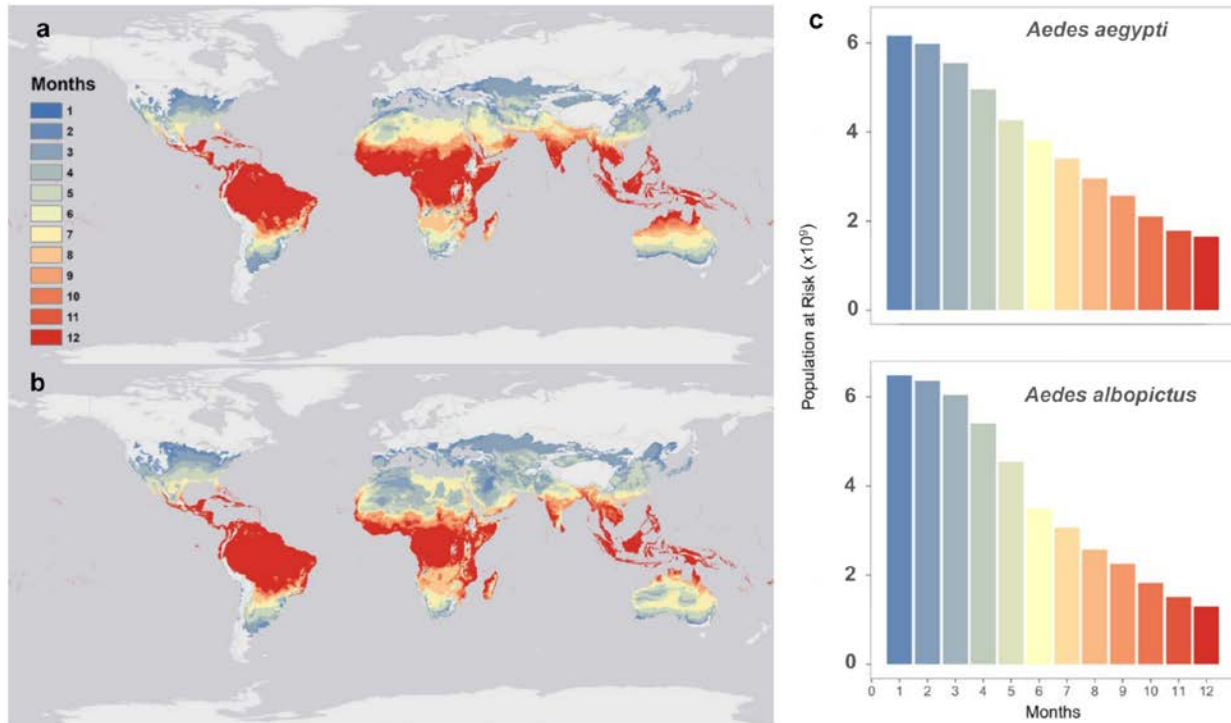
527

528

Figures and Tables

529 **Figure 1 | Mapping current transmission risk.** Maps of current monthly suitability based on
530 mean temperatures for a temperature suitability threshold corresponding to the posterior
531 probability that scaled $R_0 > 0$ is 97.5% for (a) *Aedes aegypti* and (b) *Aedes albopictus*, and (c) the
532 number of people at risk (in billions) as a function of their months of exposure for *Aedes aegypti*
533 and *Aedes albopictus*.

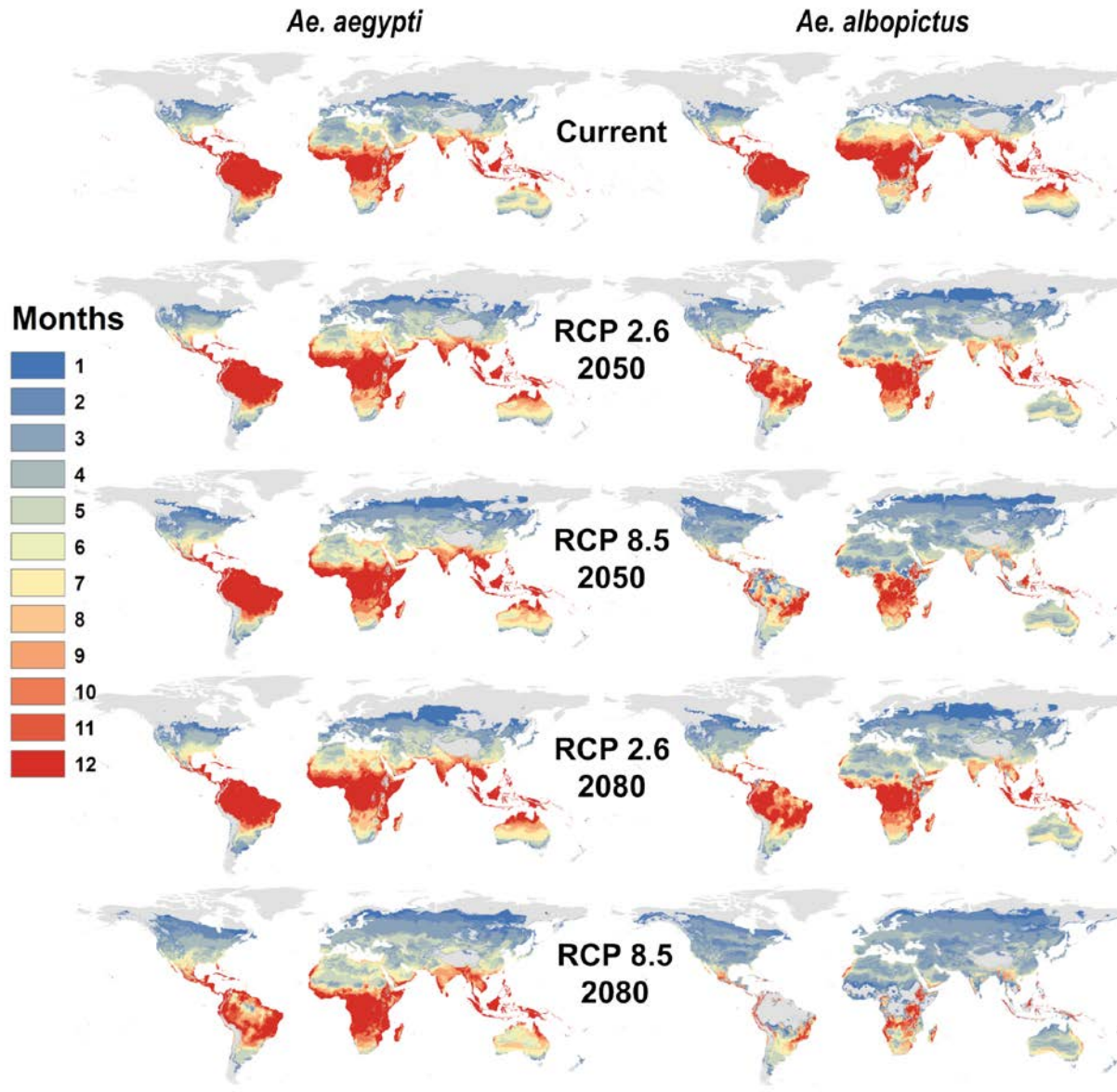
534



535

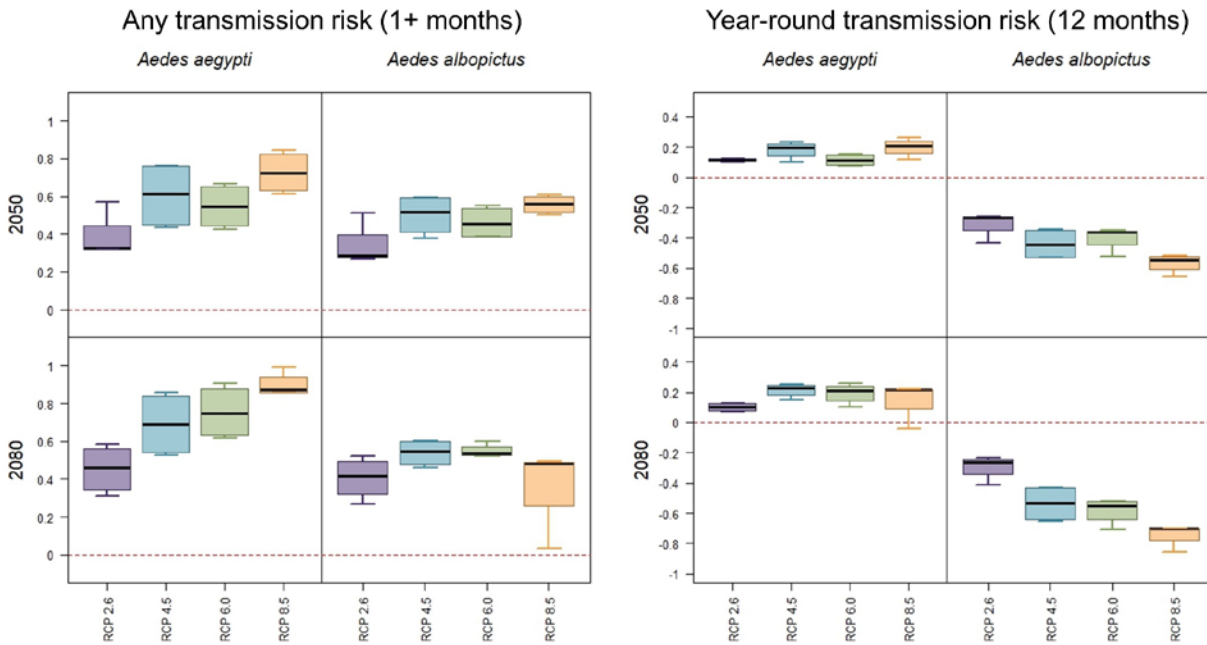
536

537 **Figure 2 | Mapping future transmission risk scenarios for *Aedes aegypti* and *Aedes***
538 ***albopictus*.** Maps of monthly suitability based on a temperature threshold corresponding to the
539 posterior probability that scaled $R_0 > 0$ is greater or equal to 97.5%, for transmission by *Aedes*
540 *aegypti* and *Aedes albopictus* for predicted mean monthly temperatures under current climate and
541 future scenarios for 2050: RCP 2.6 and RCP 8.5 in HadGEM2-ES.



542
543

544 **Figure 3 | Projected net changes in population at risk.** Projections are given as the net
545 difference in billions at risk, for *Aedes aegypti* and *Aedes albopictus* transmission, between
546 current maps and 2050 (top row) or 2080 (bottom row). Results are further broken down by
547 representative climate pathways (RCPs), each averaged across 4 general circulation models.
548



549
550
551

552 **Table 1. Changing population at risk patterns for *Aedes aegypti*.** All values are given in
 553 millions; future projections are averaged across GCMs, broken down by year (2050, 2080) and
 554 RCP (2.6, 4.5, 6.0, 8.5), and are given as net change from current population at risk. 0+/0- denote
 555 the sign of smaller non-zero values that rounded to 0.0, whereas “0” denotes true zeros.

Region	Current	2050				2080			
		2.6	4.5	6.0	8.5	2.6	4.5	6.0	8.5
Asia (Central)	69.9	8.4	10.5	9.9	12.2	8.1	11.8	12.5	15.6
Asia (East)	1,321.9	42.5	49.2	46.4	58.9	38.8	56.7	61.9	72.7
Asia (High Income Pacific)	164.0	-0.5	0+	-0.5	0.7	-0.6	0.6	1.0	1.7
Asia (South)	1,666.4	-0.1	1.6	0.7	3.7	-0.5	3.4	4.3	8.2
Asia (Southeast)	593.9	-2.1	0+	-0.6	2.3	-2.4	1.6	2.6	5.5
Australasia	12.9	3.6	5.7	5.3	6.7	4.3	6.2	6.9	8.0
Caribbean	40.4	-1.8	-1.7	-1.7	-1.6	-1.8	-1.6	-1.6	-1.5
Europe (Central)	22.7	44.2	71.8	69.0	83.3	59.0	79.3	85.5	90.6
Europe (Eastern)	41.3	57.9	110.4	93.5	133.9	80.0	124.7	130.7	156.2
Europe (Western)	114.6	47.2	132	112.0	166.8	90.3	156.4	180.8	220.9
Latin America (Andean)	31.3	2.8	3.4	3.3	4.0	2.6	3.9	4.1	5.5
Latin America (Central)	160.3	20.4	24.6	23.4	36	18.4	34.6	39.0	61.1
Latin America (Southern)	42.8	8.1	8.9	8.8	9.9	7.6	9.6	10.2	12.8
Latin America (Tropical)	181.8	19.2	19.5	19.5	19.6	18.9	19.6	19.7	19.8
North Africa & Middle East	439.5	19.7	24.1	23.8	27.2	19.3	25.9	27.3	30.3
North America (High Income)	281.9	36.2	48.3	42.6	55.0	37.8	53.6	57.1	62.8
Oceania	6.2	0.3	0.6	0.5	0.8	0.2	0.8	0.9	1.5
Sub-Saharan Africa (Central)	115.6	5.7	6.8	6.5	7.8	5.3	7.7	8.3	9.5
Sub-Saharan Africa (East)	274.8	48.8	63.7	59.1	72.2	44.7	70.8	76.6	90.9
Sub-Saharan Africa (Southern)	46.1	23.6	25.8	25.6	26.7	23.4	26.7	27.1	28.0
Sub-Saharan Africa (West)	384.0	-0.9	-0.7	-0.8	-0.7	-0.9	-0.6	-0.6	-0.4

556

557

558

559 **Table 2. Changing population at risk patterns for *Aedes albopictus*.** All values are given in
 560 millions; future projections are averaged across GCMs, broken down by year (2050, 2080) and
 561 RCP (2.6, 4.5, 6.0, 8.5), and are given as net change from current population at risk. 0+/0- denote
 562 the sign of smaller non-zero values that rounded to 0.0, whereas “0” denotes true zeros.

Region	Current	2050				2080			
		2.6	4.5	6.0	8.5	2.6	4.5	6.0	8.5
Asia (Central)	75.7	5.0	6.9	6.4	8.8	4.7	8.1	9.1	11.2
Asia (East)	1,367.0	16.1	20.8	18.9	25.2	15.0	24.0	26.5	32.4
Asia (High Income Pacific)	167.7	-2.6	-2.3	-2.6	-2.0	-2.7	-2.1	-1.9	-2.8
Asia (South)	1,673.8	-3.2	-1.7	-2.3	0+	-3.5	-0.5	-0.3	-19.1
Asia (Southeast)	602.5	-5.3	-3.8	-4.0	-6.7	-5.4	-8.5	-20.1	-124.8
Australasia	16.6	3.2	3.9	3.8	4.5	3.3	4.2	4.7	5.3
Caribbean	40.8	-1.8	-1.8	-1.8	-1.8	-1.9	-1.8	-1.8	-2.3
Europe (Central)	44.8	51.3	65.0	65.1	68.3	60.6	67.8	68.9	70.7
Europe (Eastern)	70.4	84.0	116.6	104.2	123.1	101.4	122.0	123.3	129.9
Europe (Western)	135.3	98.5	179.8	161.4	208.9	149.2	199.4	215.3	243.0
Latin America (Andean)	33.9	1.6	2.2	2.0	2.6	1.6	2.6	2.7	2.5
Latin America (Central)	179.1	21.9	27.0	27.9	31.1	17.6	29.7	30.3	23.6
Latin America (Southern)	50.4	3.2	3.6	3.6	4.8	2.8	4.2	4.9	7.6
Latin America (Tropical)	203.0	-1.5	-2.0	-1.6	-6.0	-1.5	-5.6	-8.0	-26.3
North Africa & Middle East	455.0	10.6	13.0	12.9	14.2	10.4	13.5	14.1	11.8
North America (High Income)	311.6	20.6	28.4	26.0	32.1	22.6	31.6	32.3	34.7
Oceania	6.8	0.5	0.8	0.6	1.0	0.4	0.9	1.0	0.8
Sub-Saharan Africa (Central)	120.8	2.8	3.5	3.3	4.2	2.5	4.1	4.4	-3.8
Sub-Saharan Africa (East)	320.2	30.3	39.1	36.3	42.4	27.9	41.8	42.8	34.2
Sub-Saharan Africa (Southern)	70.1	3.4	3.8	3.8	3.9	3.4	4.0	4.0	4.3
Sub-Saharan Africa (West)	384.9	-1.4	-1.5	-1.5	-2.0	-1.4	-1.9	-3.5	-59.0

563

564

565 **Table 3. Top 10 regional increases in overall transmission risk (one or more months).**
 566 Regions are ranked based on millions of people exposed for the first time to any transmission
 567 risk; parentheses give the net change (first exposures minus populations escaping transmission
 568 risk). All values are given for the worst-case scenario (RCP 8.5) in the longest term (2080).

<i>Aedes aegypti</i>		<i>Aedes albopictus</i>	
1. Europe (Western)	224 (220.9)	1. Europe (Western)	246.2 (243)
2. Europe (Eastern)	156.4 (156.2)	2. Europe (Eastern)	130.1 (129.9)
3. Sub-Saharan Africa (East)	92.8 (90.9)	3. Europe (Central)	71 (70.7)
4. Europe (Central)	90.9 (90.6)	4. Sub-Saharan Africa (East)	58.1 (34.2)
5. Asia (East)	81.7 (72.7)	5. Latin America (Central)	51.9 (23.6)
6. North America (High Income)	65.7 (62.8)	6. Asia (East)	41.4 (32.4)
7. Latin America (Central)	62 (61.1)	7. North America (High Income)	37.7 (34.7)
8. North Africa & Middle East	34.3 (30.3)	8. North Africa & Middle East	19.4 (11.8)
9. Sub-Saharan Africa (Southern)	28 (28)	9. Asia (South)	12.1 (-19.1)
10. Latin America (Tropical)	21.7 (19.8)	10. Asia (Central)	11.2 (11.2)
Total (across all 21 regions)	951.3 (899.7)	Total (across all 21 regions)	721.1 (373.9)

569

570

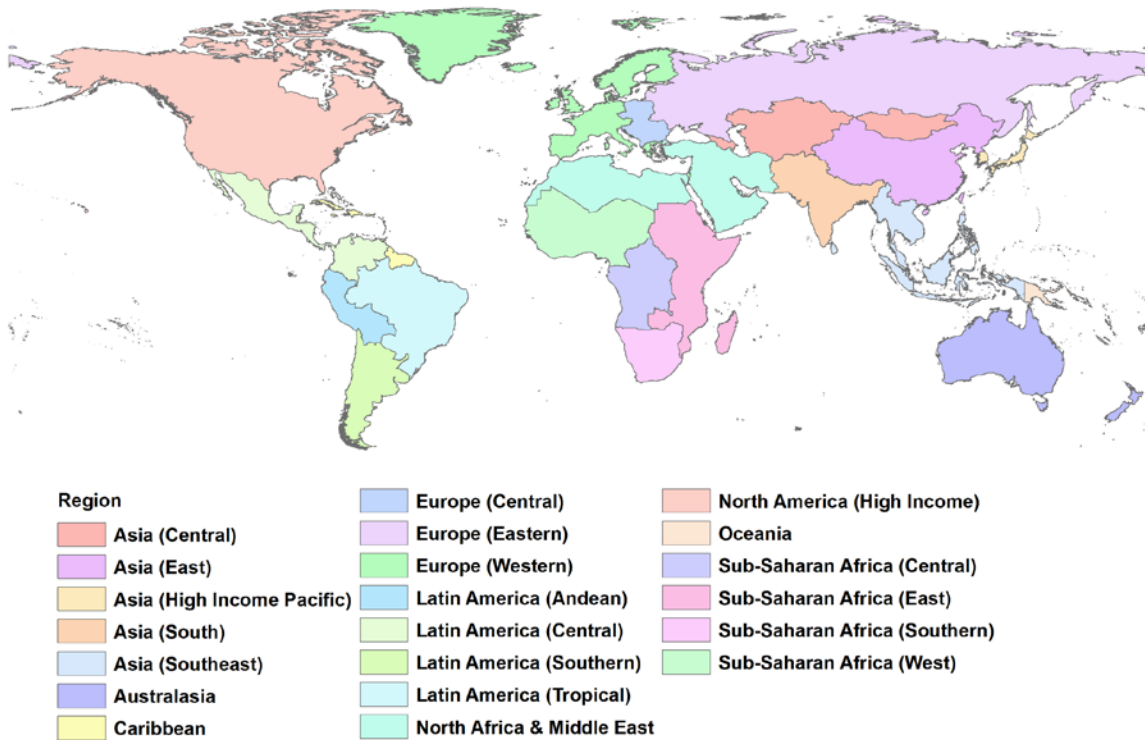
571

Supplementary Figures & Tables

572

573 **Figure S1. Global health regions.** We adopt the same system as the Global Burden of Disease
574 Study in our regional breakdown.

575



576

577 **Table S1. Changing year-round (12 month) population at risk patterns for *Aedes aegypti*.**
 578 All values are given in millions; future projections are averaged across GCMs, broken down by
 579 year (2050, 2080) and RCP (2.6, 4.5, 6.0, 8.5), and are given as net change from current
 580 population at risk. 0+/0- denote the sign of smaller non-zero values that rounded to 0.0, whereas
 581 “0” denotes true zeros. (Losses do not indicate loss of any transmission, only to reduction 11 or
 582 fewer months.).

583

Region	Current	2050				2080			
		2.6	4.5	6.0	8.5	2.6	4.5	6.0	8.5
Asia (Central)	0	0	0	0	0	0	0	0	0
Asia (East)	0+	1.4	1.8	1.1	3.7	1.6	4.5	4	8.3
Asia (High Income Pacific)	3.6	-0.2	-0.2	-0.2	-0.2	-0.2	-0.2	-0.2	-0.2
Asia (South)	286.4	21.8	71.8	13.7	73.6	12.1	89.7	72.6	29.6
Asia (Southeast)	499.4	19.2	22.4	19.9	25.1	18.9	26.3	15.4	-10.3
Australasia	0.2	0+	0+	0+	0.1	0+	0.2	0.2	0.3
Caribbean	34.8	1.8	2.2	2.1	2.8	1.7	2.6	2.9	3.3
Europe (Central)	0	0	0	0	0	0	0	0	0
Europe (Eastern)	0	0	0	0	0	0	0	0	0
Europe (Western)	0	0	0	0	0	0	0	0	0+
Latin America (Andean)	14.0	3.9	4.8	4.6	5.7	3.5	5.4	5.8	7.5
Latin America (Central)	88.1	13.0	18.8	17.0	25.8	12.0	24.4	27.4	34.1
Latin America (Southern)	0	0	0	0	0	0	0	0	0.2
Latin America (Tropical)	67.5	27.2	34.5	30.8	41.5	27.3	39	42.9	54.9
North Africa & Middle East	12.5	-5.2	-5.5	-6.0	-5.6	-4.7	-5.4	-5.4	-3.9
North America (High Income)	0.5	0.3	0.9	0.6	1.5	0.3	1.9	1.6	5.5
Oceania	0	0	0	0	0	0	0	0	0
Sub-Saharan Africa (Central)	5.3	0.3	0.6	0.4	0.9	0.3	0.7	0.9	1.7
Sub-Saharan Africa (East)	79.0	19.1	23.1	22.4	26.8	16.6	25.4	28.0	36.1
Sub-Saharan Africa (Southern)	126.9	43.8	60.7	56.7	78.3	37.9	74.3	85.5	110.3
Sub-Saharan Africa (West)	0	0+	0.1	0.1	0.3	0+	0.2	0.6	4.4

584

585

586

587 **Table S2. Changing year-round (12 month) population at risk patterns for *Aedes***
 588 ***albopictus*.** All values are given in millions; future projections are averaged across GCMs,
 589 broken down by year (2050, 2080) and RCP (2.6, 4.5, 6.0, 8.5), and are given as net change from
 590 current population at risk. 0+/0- denote the sign of smaller non-zero values that rounded to 0.0,
 591 whereas “0” denotes true zeros. (Losses do not indicate loss of any transmission, only to
 592 reduction 11 or fewer months).

593

Region	Current	2050				2080			
		2.6	4.5	6.0	8.5	2.6	4.5	6.0	8.5
Asia (Central)	0	0	0	0	0	0	0	0	0
Asia (East)	1.3	1.4	-0.4	-0.5	-1	1	-0.9	-1	-1.2
Asia (High Income Pacific)	3.6	-0.3	-0.5	-0.4	-2.9	-0.2	-2.2	-3.1	-3.6
Asia (South)	98.3	-73	-80.3	-78.9	-87.3	-67.7	-86.1	-88.5	-92.6
Asia (Southeast)	435.3	-133.9	-213.3	-190.9	-277.4	-131.9	-254.8	-282.7	-343.6
Australasia	0.2	0+	0+	0+	0-	0+	0-	0-	0-
Caribbean	39.3	-5.9	-11.7	-9.4	-17.5	-4.5	-16.1	-18.1	-28.0
Europe (Central)	0	0	0	0	0	0	0	0	0
Europe (Eastern)	0	0	0	0	0	0	0	0	0
Europe (Western)	0	0	0	0	0+	0	0+	0+	0.1
Latin America (Andean)	17.9	2	0.1	0.5	-3	1.8	-2	-3.1	-5
Latin America (Central)	97.2	-23.2	-26.8	-25.3	-31.0	-20.8	-29.3	-31.4	-33.6
Latin America (Southern)	0	0	0	0	0+	0	0	0+	0+
Latin America (Tropical)	93.6	-0.8	-5.2	-6.1	-9.7	-2.9	-10.1	-12.9	-37.1
North Africa & Middle East	2.6	0+	0+	-0.2	-0.2	0.1	0-	-0.2	-0.1
North America (High Income)	1	2.8	1.4	1	0+	1.6	0.1	-0.2	-0.2
Oceania	0	0	0	0	0	0	0	0	0
Sub-Saharan Africa (Central)	5.9	0.4	0.4	0.5	0.1	0.4	0.1	0-	-1.4
Sub-Saharan Africa (East)	96.6	8.0	5.1	6.8	-4.5	7.5	-9.1	-9.9	-45.8
Sub-Saharan Africa (Southern)	133.5	31.9	38.8	38.8	43.4	29.7	39.5	43.9	39.2
Sub-Saharan Africa (West)	0+	0+	0.5	0.4	1.8	0+	0.9	2	6.2

594

595

596 **Table S3. Top 10 regional increases in year-round transmission risk (12 months).** All
 597 calculations are otherwise the same as in Table 3.

<i>Aedes aegypti</i>		<i>Aedes albopictus</i>	
1. Asia (South)	209.9 (29.6)	1. Sub-Saharan Africa (East)	114.3 (39.2)
2. Sub-Saharan Africa (East)	152.6 (110.3)	2. Latin America (Tropical)	39.7 (-37.1)
3. Latin America (Tropical)	63.2 (54.9)	3. Latin America (Central)	38.1 (-33.6)
4. Asia (Southeast)	44 (-10.3)	4. Sub-Saharan Africa (Central)	23.1 (-45.8)
5. Latin America (Central)	40.7 (34.1)	5. Asia (Southeast)	16.3 (-343.6)
6. Sub-Saharan Africa (Central)	36.6 (36.1)	6. Latin America (Andean)	8.6 (-5)
7. Sub-Saharan Africa (West)	8.7 (-130.2)	7. Sub-Saharan Africa (Southern)	6.2 (6.2)
8. Asia (East)	8.3 (8.3)	8. Sub-Saharan Africa (West)	2.5 (-194)
9. Latin America (Andean)	8 (7.5)	9. North Africa & Middle East	2.4 (-0.1)
10. North Africa & Middle East	7.4 (-3.9)	10. Oceania	2 (-1.4)
Total (across all 21 regions)	597.2 (151.6)	Total (across all 21 regions)	256.5 (-740.8)

598